# Supporting Information

Kaehr et al. 10.1073/pnas.1205816109

## SI Text

**SI Methods.** ***Cell culture and chemical fixation.*** Cell culture was performed using standard procedures (atcc.org). Briefly, AsPC-1 (CRL-1682), 4T1 (CRL-2539), CHO (CCL-61), 3T3 (CCL-92), and B16-F1 (CRL-6323) were obtained from American Type Culture Collection (ATCC) and maintained in media containing 10% FBS at 37 °C and 5% $CO_2$. Cells were passaged at approximately 80% confluency. Red blood cells were obtained from Biological Specialty Corporation and maintained as shipped in heparin (product no. 235-11) until fixed. RBL-2H3 cells were generously provided by Prof. Diane Lidke, Department of Pathology and Cancer Research and Treatment Center, University of New Mexico, Albuquerque, NM 87131, USA. Priming of IgE receptors was achieved by incubation with anti-dinitrophenyl (DNP)-IgE (1 mg/mL) for approximately 20 h. Following rinsing, cells were activated by incubating with antigen (1 mg/mL polyvalent DNP-BSA) for 10 min at 37 °C.

For fixation, cells in media were rinsed in PBS (pH 7.4) and incubated in 2–4% formaldehyde or glutaraldehyde in PBS for a minimum of 10 min, followed by rinsing in PBS.

***Silicification of mammalian cells.*** Cells differentiated on substrates were incubated in a closed container of 100 mM tetramethyl orthosilicate (TMOS) solution in 1 mM HCl at approximately 40 °C for 16–18 h. Cell/silica composites (CSCs) were dehydrated by sequential soaking in deionized (DI) water, 1:1 DI water: methanol, and 100% methanol (2X) for 10 min in each solution. CSC particles were derived similarly by incubating cell suspensions in TMOS on a shaker. For rinsing and drying, cells were pelleted and redispersed sequentially in rinse solutions (described above) and finally air-dried overnight from 100% methanol. For the nonsilicified cell shown in Fig. 3, samples were fixed in 4% gluteraldehyde/PBS (vol/vol) solution for 30 min and dehydrated by using 10-min long sequential washes [10% EtOH in $H_2O$, 33% EtOH, 50% EtOH, 66% EtOH, 2x 100% EtOH, 1:1 EtOH, hexamethyldisilazane (HMDS), 100% HMDS, and allowed to air dry overnight]. Calcination was performed in air at 550 to 600 °C for 3–4 h, which eliminated the majority of organics. Fig. S9 shows a representative thermogravimetric analysis (TGA) curve acquired from CHO-derived CSCs.

***Optical SEM and energy dispersive spectroscopy (EDS).*** Optical images (Fig. 1 *B* and *C*, Fig. 2 *A*, *Right* , and Fig. 5*C*) were acquired on an inverted Nikon microscope (Eclipse TI) equipped with differential interference contrast and florescence optics. Images were captured using an Andor Ixon electron multiplying charge coupled device. Confocal images in Fig. 5 *A* and *B* were acquired using a Zeiss LSM 510-Meta confocal. All SEM images were recorded using an FEI Quanta series scanning electron microscope. This instrument was equipped with an EDS from EDAX which was used in multipoint mode for elemental analysis of samples. SEM images shown in Figs. 1–4 were sputter-coated with gold to a thickness of 10 nm.

***Surface area and porosity measurements.*** Nitrogen adsorption data for calcined CSCs derived from CHO cells silica was collected with a Micromeritics ASAP 2020 porosimetry analyzer, with surface area and pore size distribution calculated using Brunauer–Emmett–Teller (BET) analysis and a density functional theory (DFT) model for cylindrical pores in an oxide material, respectively.

***Lipid bilayer functionalization, enzyme activity, and silica localization.*** Liposomes consisting of 60% 1,2-dioleoyl-sn-glycero-3-phosphocholine, 30% Cholesterol, 5% 1,2-dioleoyl-sn-glycero-3-phosphoethanolamine, and 5% PEG2000 PE (Avanti Polar Lipids) were produced by extrusion through a 0.1 μm filter to produce liposomes of approximately 110 nm in diameter. Lipid bilayers were deposited on the surface of CSCs by mixing with liposomes for a minimum of 30 min at approximately 40 °C. Lipid bilayer and nuclei staining were achieved using CellMask orange and 4′,6-diamidino-2-phenylindole dihydrochloride (DAPI), respectively (Invitrogen no. C10045 and S33025). Nonspecific esterase activity was determined by incubation of particles with 5 μM CellTracker Green 5-Chloromethylfluorescein Diacetate (Invitrogen no. C2925; used to determine viability and track cell generations) in PBS (pH 7.4) at room temperature. Silica deposition was imaged using 100 ng•$mL^{-1}$ of PDMPO ([2-(4-pyridyl)-5-((4-(2-dimethylaminoethylamino-carbamoyl)methoxy)phenyl)oxazole]) (Invitrogen Corp.) of the fluorescent indicator incorporated into the silicification solution, following extensive rinsing in PBS.

***Electrical characterization of carbonized cells.*** For electrical measurements, particles were placed onto gold coated coverslips and IV curves were performed using a one-probe nanomanipulator retro-fit inside of a JEOL 6701F scanning electron microscope. Current and voltage are measured and controlled between the probe and substrate using an Agilent B1500A semiconductor device analyzer. Probe tips are polycrystalline tungsten wire electrochemically etched to an end radius of curvature of less than 250 nm.

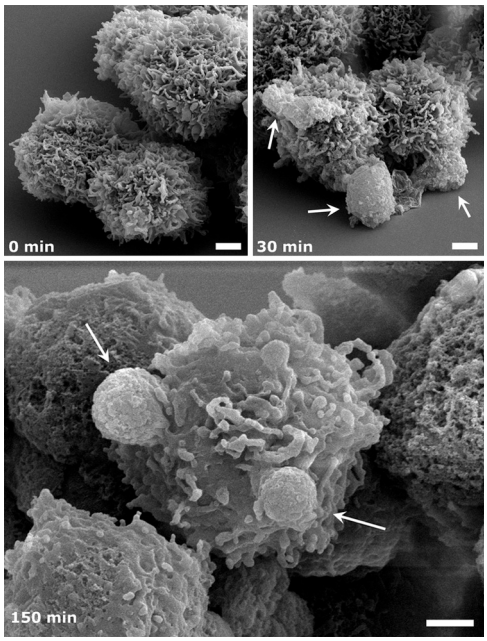


**Fig. S1.** Clusters of calcined (500 °C, 3 h) silica replicas templated from 4T1 cells incubated in 5 μm doxorubicin to induce apoptosis. Arrows denote apoptotic blebs. Filamentous surface structures appear to degrade over the 150 min incubation. (Scale bars, 2 μm.)

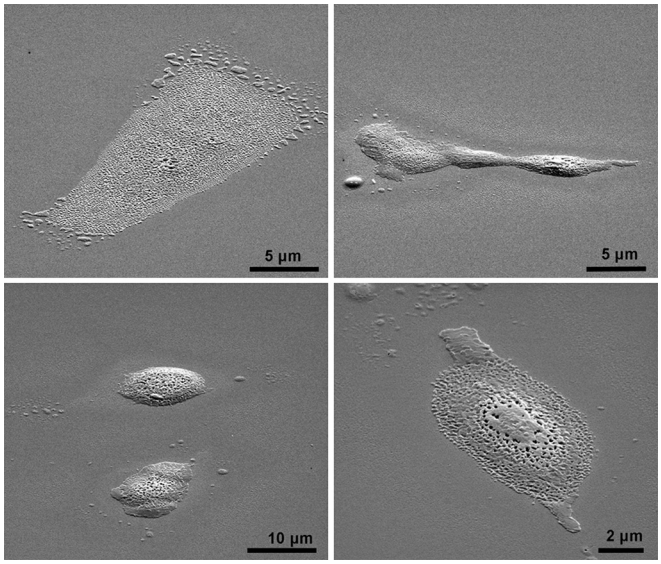


**Fig. S2.** Calcination of fixed AsPC-1 cells in the absence of silicic acid treatment.

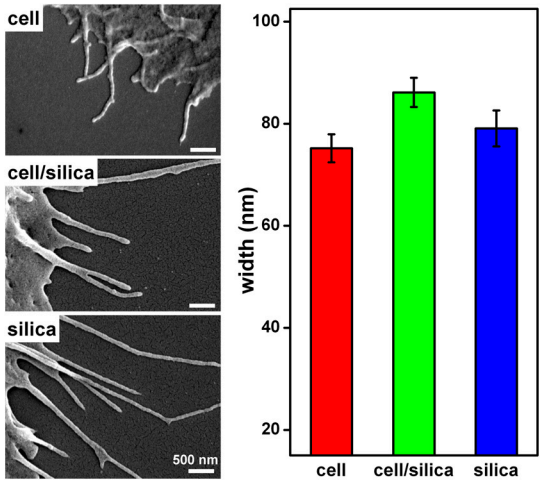


**Fig. S3.** SEM analysis of filopodia mean width of fixed cells (75 nm), cell/silica composites (86 nm), and silica (79 nm) derived from substrate-bound differentiated AsPC-1 cells show a significant difference in mean width (at 0.05 level using overall ANOVA, $n > 15$ per sample). The cell sample was prepared using EtOH : HMDS sample preparation as described in *SI Methods*. Error bars indicate the standard error of the mean.

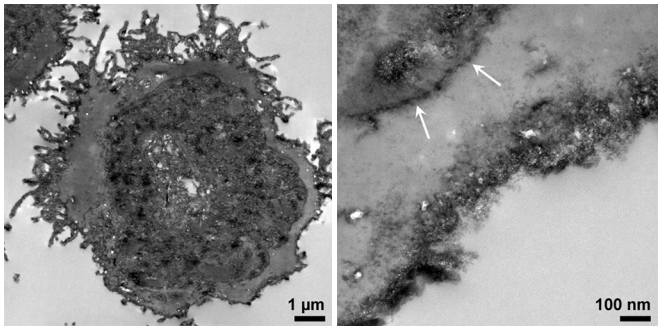


**Fig. S4.** Unstained transmission electron microscopy cross-section of 4T1- derived CSC showing high contrast at the outer and nuclear membrane (arrows) attributed to areas of high silica concentration.

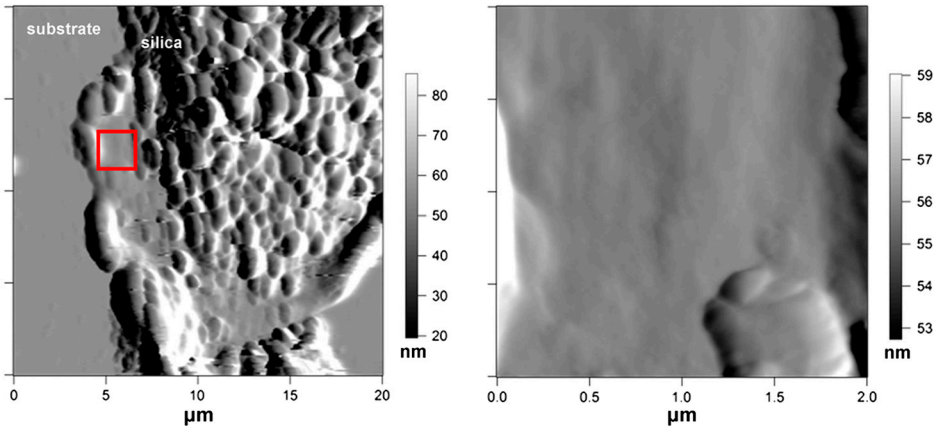


**Fig. S5.** Atomic force microscopy images of the external surface of a calcined CSC derived from ASPC-1 cells. Analysis of the height image (*Right*, scanned area of the red box in the *Left*) was used to measure surface roughness (standard deviation, $\sigma = 1$ nm) within error attributed to the tip radius (<2 nm).

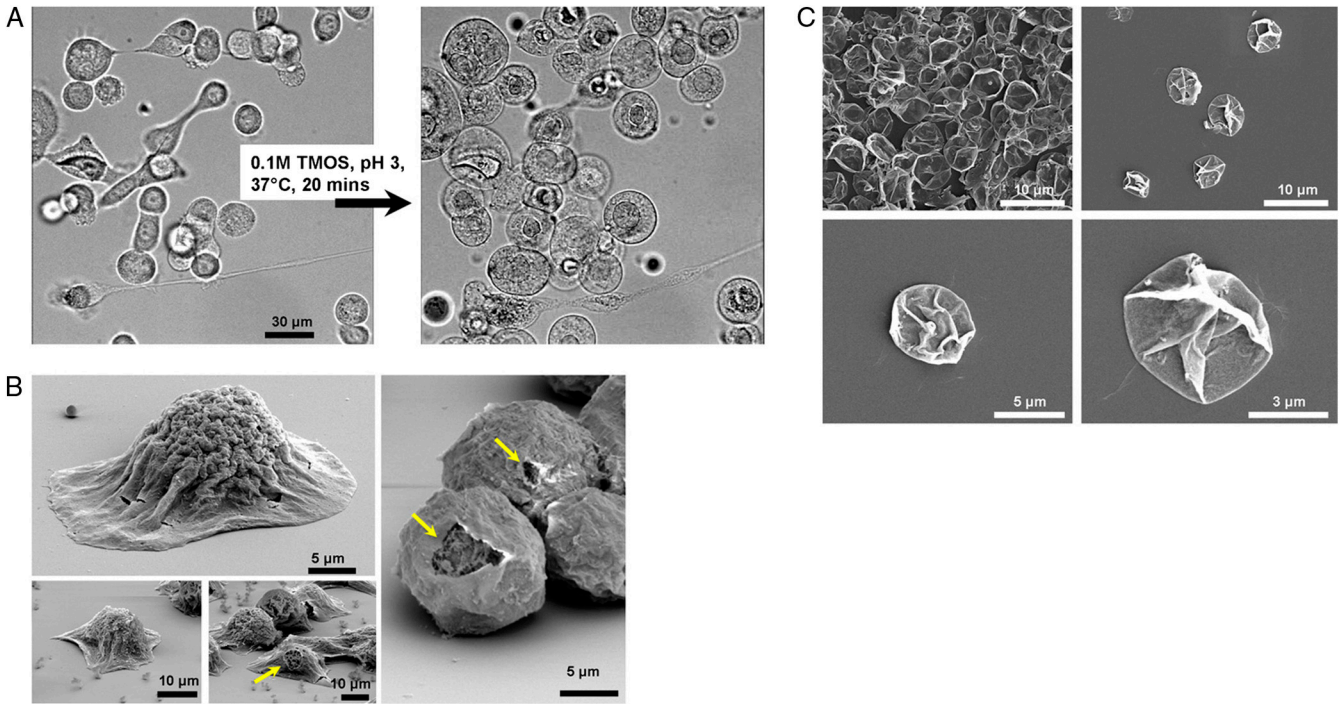


**Fig. S6.** (*A*) Silicification of cells (AsPC-1) without chemical fixation results in cell swelling indicative of hypoosmotic cellular stress. (*B*) Calcined samples (AsPC-1, *Left*; 4T1-particles, *Right*) show resultant cell templated silica with altered morphology. Yellow arrows indicate areas of membrane rupture. (*C*) Silicification of fixed erythrocytes induces cell lysis resulting in silica templated by erythrocyte membranes following calcination.

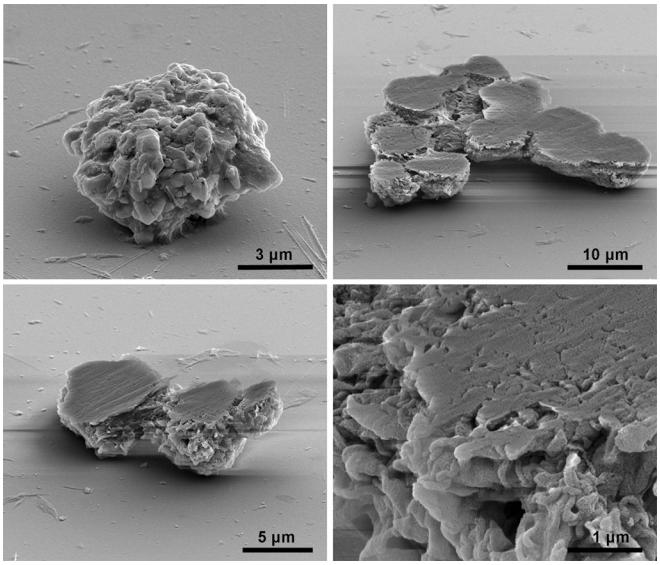


**Fig. S7.** Incubation of 4T1 cells in 0.5% Triton X-100 prior to silicification results in CSCs with altered surface morphologies and flattened regions most likely incurred from settling in the silicification reaction vessel.

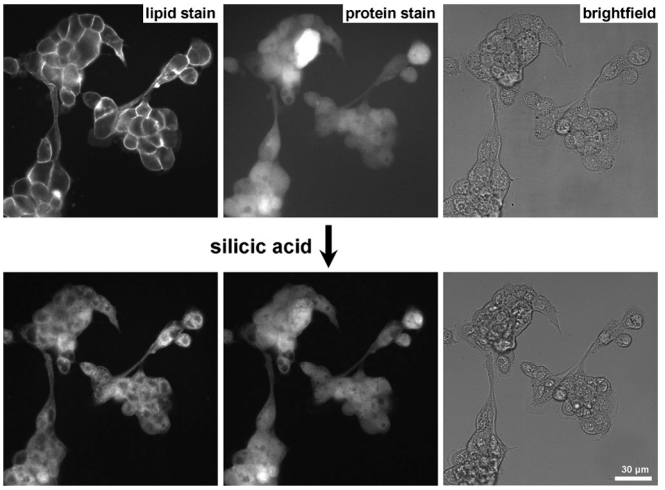


**Fig. S8.** AsPC-1cells fluorescently stained for outer membrane (CellMask Orange) and cytoplasmic proteins (CellTracker Green) before silicification (*Top*) show loss of membrane dye localization whereas the protein dye remained stationary. Membrane staining of cells following silicification produced qualitatively similar results.

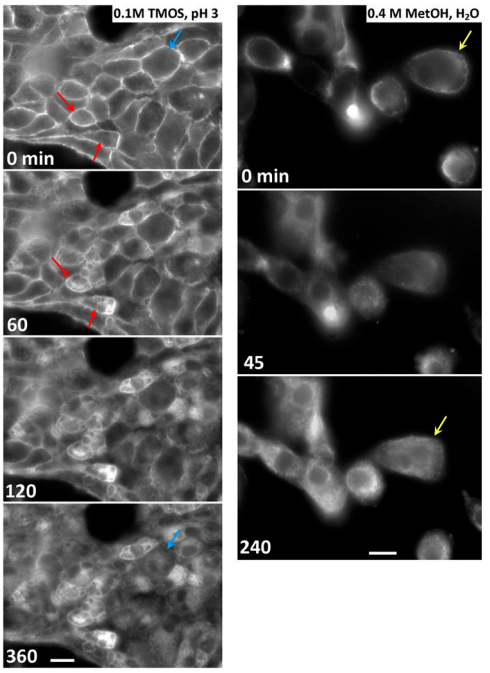


**Fig. S9.** Time-lapse imaging of fixed AsPC-1 cells fluorescently stained for outer membrane (CellMask Orange) under silicification conditions (*Left*) and methanol (*Right*) both at 37 °C. Delocalization of fluorescent dye from the cell exteriors with concurrent increase in interior fluorescence indicates that the timescale for membrane permeabilization varies from cell to cell, occurring over minutes (red arrows) to hours (blue arrows). Similar observations in 0.4 methanol (yellow arrow) indicate membrane permeabilization is primarily due to incubation in methanol generated from the acid catalyzed hydrolysis of the silicic acid precursor TMOS. (Scale bars, 10 μm.)

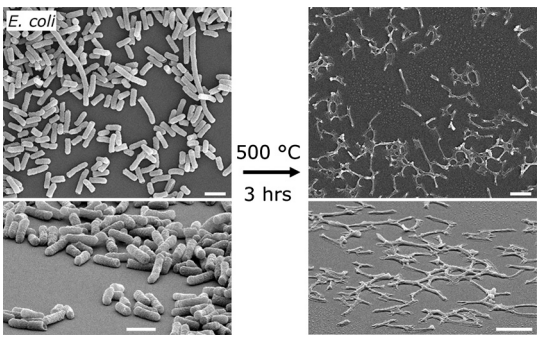


**Fig. S10.** SEM images of Gram-negative bacterial cells (*Escherichia coli*) silicified using identical conditions to those of mammalian cells (100 mM silicic acid, pH 3) indicates that following calcination (*Right*) cellular-structure (*Left*) is not stabilized (via intracellular silicification) and thus obliterated following calcination (*Right*). (Scale bars, 2 μm.)

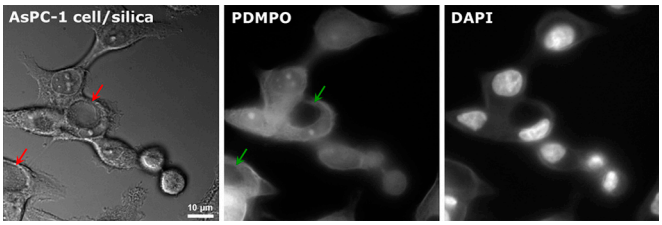


**Fig. S11.** Brightfield (*Left*) and epifluorescence (*Middle and Right*) images of AsPC-1 cell/silica shows silica localization (PDMPO) throughout the cellular interior—including the nucleus (DAPI)—with the noticeable exception of vacuole-type structures (red and green arrows).

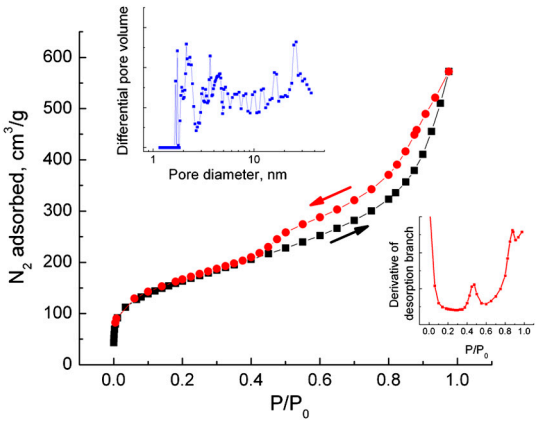


**Fig. S12.** $N_2$ sorption isotherm of calcined CSCs templated from CHO cells. The lack of a distinct condensation step in the adsorption branch indicates a wide pore size distribution (PSD); a fit to the adsorption branch using a hybrid DFT model for cylindrical pores in silica (1) (*Top Inset*) shows that the material contains a broad range of pore dimensions, although with no microporosity (pore size less than 2 nm). Because there is no plateau in the adsorption branch at high $P/P_0$, the total porosity for pores greater than *ca.* 40 nm cannot be determined from this isotherm. However, hysteresis in the desorption branch—likely due to a bottleneck structure within a pore network—contains two inflection points (derivative included as bottom inset) at $P/P_0 = 0.46$ and 0.87, which is indicative of two populations of internal porosity.

1 Jaroniec M, Kruk M, Olivier JP, Koch S (1999) A New Method for the Accurate Pore Size Analysis of MCM -41 and Other Silica Based Mesoporous Materials , *Fifth International Symposium on the Characterization of Porous Solids* (COPS V), eds. Unger KK, Kreysa G, Baselt JP (Elsevier, Heidelburg), pp 71–80.

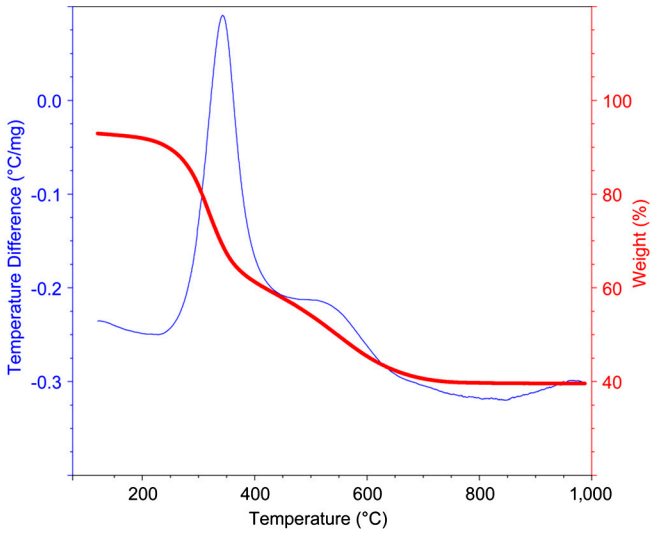


**Fig. S13.** Representative TGA (red) and differential thermal analysis (blue) profiles for 7 mg of CHO-derived CSCs (ramp rate, 10 °C/ min).